Double aromaticity in transition metal centered double-ring boron clusters M@B2n (M = Ti, Cr, Fe, Ni, Zn; n = 6, 7, 8)

Chang Xu, Longjiu Cheng, and Jinlong Yang

Citation: The Journal of Chemical Physics **141**, 124301 (2014); doi: 10.1063/1.4895727
View online: http://dx.doi.org/10.1063/1.4895727
View Table of Contents: http://scitation.aip.org/content/aip/journal/jcp/141/12?ver=pdfcov
Published by the AIP Publishing

THE JOURNAL OF CHEMICAL PHYSICS **141**, 124301 (2014)

Double aromaticity in transition metal centered double-ring boron clusters $M@B_{2n}$ (M = Ti, Cr, Fe, Ni, Zn; $n = 6, 7, 8$)

Chang Xu (徐畅),[1,2] Longjiu Cheng (程龙玖),[2,a] and Jinlong Yang (杨金龙)[1,a]
[1]*Hefei National Laboratory for Physics Sciences at the Microscale, University of Science and Technology of China, Hefei, Anhui 230026, People's Republic of China*
[2]*Department of Chemistry, Anhui University, Hefei, Anhui 230601, People's Republic of China*

(Received 22 July 2014; accepted 3 September 2014; published online 22 September 2014)

It is well known that double-ring boron clusters have got the special double aromaticity with delocalized π orbitals in two directions (tangential and radial), which are potential ligands centered by a transition metal. In this article, the transition metal centered double-ring boron clusters $M@B_{2n}$ (M = Ti, Cr, Fe, Ni, Zn; $n = 6, 7, 8$) are theoretically investigated by density functional theory calculations. These endohedral compounds have also got double aromaticity in both tangential and radial directions. Interestingly, the tangential delocalized π orbitals of boron ligands following the Huckle's $(4n + 2)$ rule do not interact with the central metal, while the radial π orbitals of boron ligands are bonded with the central mental to form *spd*-π endohedral bonding. The *spd*-π endohedral bonding follows the 18e-principle in $Ni@B_{14}$ and $Fe@B_{16}$. However, due to the flat shape of the compounds, 14e ($Cr@B_{14}$) and 16e ($Ni@B_{12}$) can also be electronically very stable where the energy levels of the *spd*-π orbitals delocalized in *z*-direction rise up. This intriguing bonding model makes sense in further study of the boron chemistry. *© 2014 AIP Publishing LLC*. [http://dx.doi.org/10.1063/1.4895727]

I. INTRODUCTION

The organo-iron compound dicyclopentadienyliron $Fe(C_2H_5)_2$ was first obtained by Kealy and Pauson[1] and Miller, Tebboth, and Tremaine[2] in 1950s. Soon after that, Wilkinson *et al.*[3] and other investigators[4,5] identified its sandwich structure and named it ferrocene. This discovery had attracted considerable attention because of its particular chemical bonding and potential application in the field of chemistry. Since then, numerous ferrocene analogues, which were called metallocenes, had been synthesized and theoretical studies revealed that the ligands of these complexes had got delocalized π bonding in common.[6–43] At first, metallocenes with organic ligands held most of the interests of researchers.[6–21] However, the reports on the inorganic ligands, which were found have the similar delocalized bondings, had grown rapidly since the beginning of 21st century.[22–43]

In recent years, all-boron clusters were considered as potential new inorganic ligands because of their aromatic and antiaromatic electronic properties similar to the hydrocarbons. Wang *et al.*[44–54] carried on a series studies on the boron clusters and complexes with boron ligands and reviewed the structure and stability of B_n ($n = 3$–20) clusters. The 2D–3D structural transition of neutral boron cluster occurs at B_{20}, of which the double-ring tubular structure is proved to be the most stable.[51,55,56] The charge effect has also affected the geometrical transition,[57] and anionic boron cluster remains planar or quasi-planar up to B_{24}^-.[58] But there are still exceptions, recent studies report a flat cage B_{14} cluster[59] and a disk-aromatic bowl cluster B_{30}.[60] Chemical bonding analysis reveals that delocalized multicenter-two-electron (*n*c-2e) σ and π bonds in all boron system stabilize the clusters, which makes the formation of metal-doped boron cluster available.[56] The boron-ligand metal compounds of wheel-type[61–65] and bowl-shape[66,67] have been reported. Cheng and Yuan[68] state the ferrocene-like sandwich complexes $Cr(B_{12})_2$, and the *spd*-π interaction between Cr and boron ligand is investigated. Recently, Popov *et al.*[69] reports the metal-doped boron complexes CoB_{12}^- and RhB_{12}^- with half-sandwich-type structure, and theoretical study reveals that there are three M-B single σ bonds and one delocalized π bond between the metal and the B_{12} ligand.

The all boron cluster B_{20} with special double-ring structure was first reported by Kiran *et al.*[55] in 2005. Molecule orbital analysis reveals that this kind of boron clusters has got strong aromaticity due to the doubly directional delocalized π orbitals.[70–73] Thus, the delocalized π orbitals in double-ring boron clusters can also interact with trans-metals. However, when centered by a trans-metal, the bonding model between the doubly delocalized π orbitals and the metal orbitals remains unclearly. In this article, the compounds of boron double-ring ligand centered with a trans-metal atom $M@B_{2n}$ (M = Ti, Cr, Fe, Ni, Zn, $n = 6, 7, 8$) are investigated using density functional theory (DFT) method. Although the global minimum structure of small bare B_n cluster ($n \leq 20$) is planar or quasi-planar in the early study,[51,55,56] the interaction with the central metal atoms helps the complexes achieve stability in double-ring formation. The structural stability is discussed and the analysis of electronic properties proved that the *spd*-π interaction plays an important part in stabilizing the $M@B_{2n}$.

---

[a] Author to whom the correspondence should be addressed. Electronic addresses: clj@ustc.edu and jlyang@ustc.edu.cn.

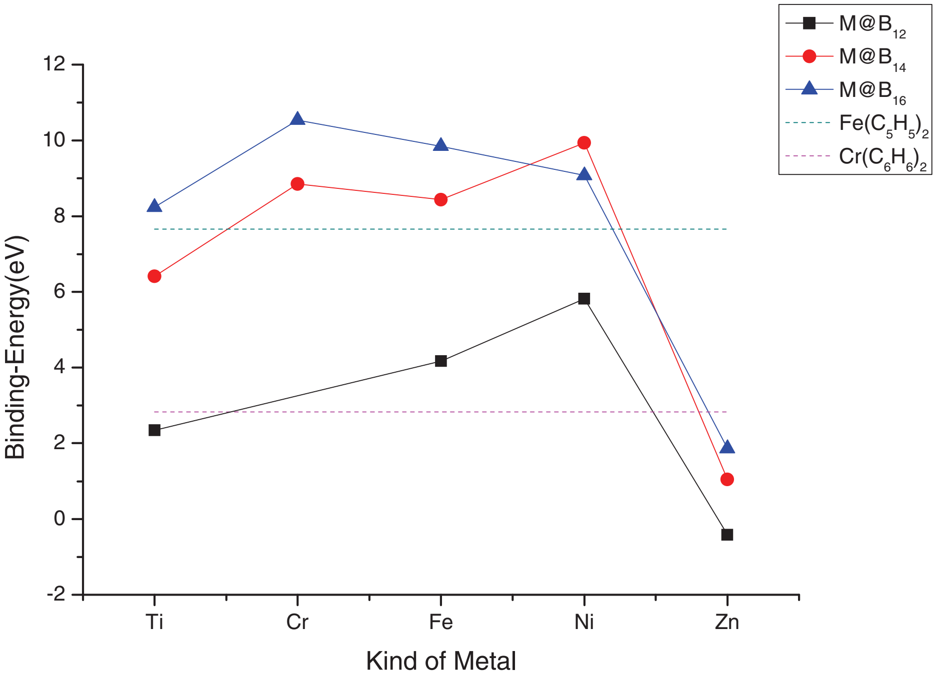

FIG. 1. Binding-Energy of $M@B_{2n}$ (M = Ti, Cr, Fe, Ni, Zn, $n = 6, 7, 8$) with $Fe(C_5H_5)_2$ and $Cr(C_6H_6)_2$ as reference.

II. COMPUTATIONAL DETAILS

In this article, the TPSSh functional[74] is chosen in the theoritcal study, which has been proved to be reliable in the study of metal-doped boron clusters.[68,75,76] The geometry optimizations are carried out with 6-31G* basis set for boron and LANL2DZ for trans-metal atoms. To confirmed the stability of the complexes, the binding energy, HOMO-LUMO gap, vertical electron affinity (VEA), vertical ionization potential (VIP), and vibrational frequency are also calculated on the TPSSh/6-31G*/LANL2DZ level of theory. The binding energy is defined as $E_b = E(M) + E(B_{2n}) - E(M@B_{2n})$ in this study. The VEA = $E(M@B_{2n}) - E(M@B_{2n}^{-})$ and VIP = $E(M@B_{2n}^{+}) - E(M@B_{2n})$ are calculated as the vertical electron affinity and vertical ionization potential. All calculations are carried out by using the GAUSSIAN 09 package,[77] and molecular orbital (MO) visualization is performed by Molekel 5.4.[78]

III. RESULTS AND DISCUSSION

A. Structure and stability

$M@B_{2n}$ clusters are optimized from ideal D_{nd} symmetry. All the compounds keep the metal centered double-ring structures except $Cr@B_{12}$, which distorts seriously after optimizing possibly due to the geometry effect. The binding energies of these compounds are shown in Figure 1 and the binding energies of two classical metallocenes, $Fe(C_5H_5)_2$ and $Cr(C_6H_6)_2$, are chosen as references. It is shown that the $Ti@B_{2n}$ and $Zn@B_{2n}$ have relative low binding energy. On one hand, as the atomic radius of Ti is the largest of the trans-metals in our study, it may not be suitable for the radius of boron double-ring, so the stability of $Ti@B_{2n}$ is weakened. Another evidence is that the binding energy increases as the size of double-ring getting bigger. On the other hand, Zn shows some inertness in forming the complexes because its 4*s* and 3*d* orbital is fulfilled with 12 electrons ($3d^{10}4s^2$), so *spd*-π interaction in the $Zn@B_{2n}$ is weakened and it gets the lowest binding energy. What is more, taking the hexatomic double-ring complexes $M@B_{12}$ into consideration, we find that only the $Ni@B_{12}$ gets the high binding energy in this series. That is because the radius of Ni atom is relative small in this trans-metal period, which could be suitable for the small ring size in $M@B_{12}$. So, the $Ti@B_{2n}$, $Zn@B_{2n}$, $Cr@B_{12}$, and $Fe@B_{12}$ are eliminated in the further study.

Then the symmetry, binding energy, HUMO-LOMO gap, vertical electron affinity (VEA), and vertical ionization potential (VIP) of the rest compounds are listed in Table I. $Ni@B_{12}$, $Cr@B_{16}$, $Fe@B_{16}$, and $Ni@B_{16}$ lost their D_{nd} symmetry due to the John-Teller effect. The large binding energy (6.16–10.37 eV) and HUMO-LOMO gap (1.14–2.36 eV) indicate the stability of these complexes, except the $Fe@B_{14}$ and $Ni@B_{16}$ with the low HUMO-LOMO gap of 0.33 eV and 0.84 eV, respectively. The low VEA and high VIP values

TABLE I. The point group, binding energy, HOMO-LUMO gaps, vertical electron affinities (VEAs), and vertical ionization potentials (VIPs) of $Ni@B_{12}$, $Cr@B_{14}$, $Fe@B_{14}$, $Ni@B_{14}$, $Cr@B_{16}$, $Fe@B_{16}$, and $Ni@B_{16}$ using TPSSh/6-31G*/LANL2DZ method.

	Point Group	E_b/eV	E_{H-L}/eV	VEA/eV	VIP/eV
$Ni@B_{12}$	C_{6v}	6.16	2.13	2.03	8.29
$Cr@B_{14}$	D_{7d}	8.85	2.02	2.36	8.27
$Fe@B_{14}$	D_{7d}	8.44	0.33	3.22	6.18
$Ni@B_{14}$	D_{7d}	9.94	2.36	1.00	7.34
$Cr@B_{16}$	C_2	10.37	1.43	2.28	7.28
$Fe@B_{16}$	C_2	9.57	1.14	1.99	6.40
$Ni@B_{16}$	C_1	10.36	0.84	2.05	6.60

confirm their stability. The calculated vibrational frequencies of the low-energy isomers are verified to be all positive, so they are true local minima.

B. Electronic structures

A recent study[79] reveals that the double-ring B_{2n} ($n = 6$–14) clusters have two directional delocalized orbitals. For even n, there are $4m + 2$ electrons in both radial and tangential delocalized orbitals following the Huckle's rule, respectively, implying the double aromaticity; for odd n, there are $4m + 2$ electrons in tangential or radial orbitals alternatively and the rest orbitals are occupied with $4m$ electrons, which indicate the complexes are in conflicting aromaticity. As a result, the B_{12}, B_{16}, B_{20}, B_{24}, and B_{28} are doubly aromatic, while B_{14}, B_{18}, B_{22}, and B_{26} have both aromaticity and antiaromaticity.

When a trans-metal is doped in the double-ring, orbitals of the metal would interact with the delocalized orbitals of boron clusters. However, there are both tangential and radial directions of π orbitals in boron double-ring. Then, which direction of the orbitals would interact with the metal? In order to get insight of the structure stability of these metal doped double-ring complexes, further studies are carried on using canonical molecular orbital (CMO) analysis. Moreover, adaptive natural density partitioning (AdNDP) method,[80,81] which has been developed for analyzing the multicenter bonds, is adopted here to identify the special bonding styles in the complexes. All these calculations are carried out on the TPSSh/6-31G*/LANL2DZ level. From the results of the electronic structures analysis, we suppose that all the five stable compounds (Ni@B_{12}, Cr@B_{14}, Ni@B_{14}, Cr@B_{16}, and Fe@B_{16}) could be classified into three categories.

Ni@B_{14} and Fe@B_{16} are included in the category I. CMO results in Figure 2(a) indicate that there are 12 delocalized orbitals in the Ni@B_{14} system, three of which are π orbitals in tangential direction and the rest nine are delocalized in radial direction. The tangential π orbitals are fulfilled with six valence electrons and follow the Huckel's ($4n + 2$) rule. But what is the origin of the radial delocalized orbitals? For all boron cluster B_{14}, former study[79] reveals that there are six electrons in the three tangential delocalized π orbitals and eight electrons in four radial delocalized orbitals. In the Ni@B_{14} complex, as Ni has ten valence electrons, we suppose the radial delocalized orbitals in B_{14} ligand could interact with Ni to form the *spd*-π delocalized molecular orbitals. So these *spd*-π orbitals would be occupied with 18 valence electrons, which follow the 18-electrons principle to make the complex stable.

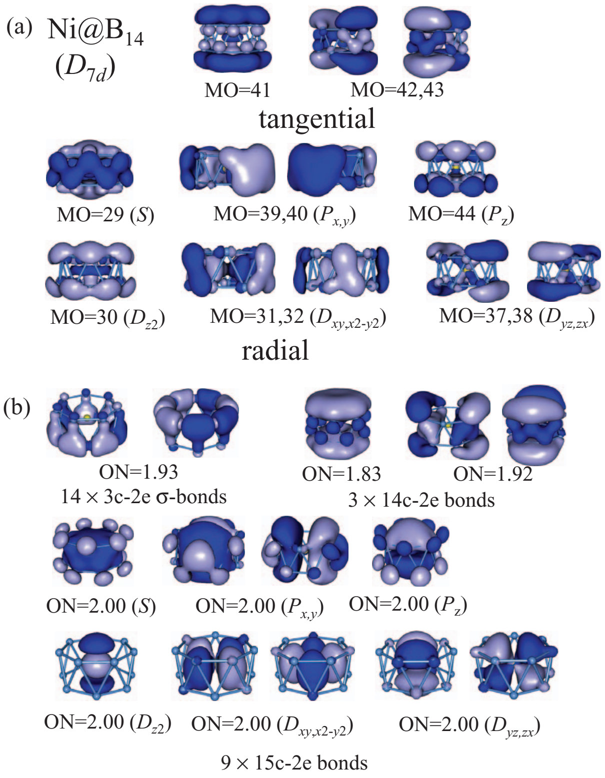

FIG. 2. (a) Canonical molecular orbitals and (b) AdNDP localized bonding patterns of Ni@B_{14}. The molecular orbital energy level (MO) is marked below each orbital (there is some overlap between the energy levels) and occupy number (ON) is marked below each bond. B is labeled blue, Ni is labeled yellow.

To confirm our inference, chemical bonding analyses of Ni@B_{14} are given by AdNDP method. There are 52 valence electrons altogether in this cluster (ten from Ni and three from each boron). Figure 2(b) reveals that there are fourteen 3c–2e BBB bonds, three 14c–2e delocalized bonds, and nine delocalized 15c–2e bonds. The bonding model of these 3c–2e bonds are in accordance with the BBB bonds in all boron clusters B_{14} and B_{14}^{2+},[70,79] which indicates that these 3c–2e bonds do not interact with the central Ni. Compared with the CMO results, it is clearly shown that the three 14c–2e bonds are delocalized π orbitals in the tangential direction, which almost have no contribution for the Ni–B_{14} endohedral bonding. From the orbital symmetry of the nine delocalized bonds, these 15c–2e orbitals can be clearly viewed as super S, $P_{x,y,z}$, and $D_{xy,yz,xz,x2\text{-}y2,z2}$ orbitals (Figure 2(b)). Thus, they are formed by the *spd*-π interaction between the radial delocalized orbitals in boron ligand and the outer *spd* orbitals in Ni, which confirms our inference. As these orbitals are fulfilled with 18 valence electrons ($S^2P^6D^{10}$), the Ni@B_{14} system forms the closed-shell spherical structure and follows the 18-electron principle to reach high stability. The large binding energy (9.94 eV), HUMO-LOMO gap (2.36 eV) and VIP (7.34 eV), and small VEA (1.00 eV) are the other evidence, which implies the Ni@B_{14} is a "magic number" in these series of complexes (Table I).

Fe@B_{16} has the similar electronic structure with Ni@B_{14} due to the same number of delocalized electrons. The CMO results plotted in Figure 3 reveal that there are three delocalized π orbitals with six valence electrons in tangential direction and nine *spd*-π delocalized orbitals (S, $P_{x,y,z}$, and $D_{xy,yz,xz,x2\text{-}y2,z2}$) with 18 electrons in radial direction. So it also obeys the Huckel's ($4n + 2$) rule and 18-electrons principle in two directions, respectively.

Category II includes Cr@B_{14}. Its number of delocalized electrons is four less than the clusters in category I. In Figure 4(a), CMO analysis reveals that there are three delocalized π orbitals in the tangential direction and seven delocalized orbitals in the radial direction. The tangential π orbitals are occupied with six valence electrons, following the Huckel's rule.

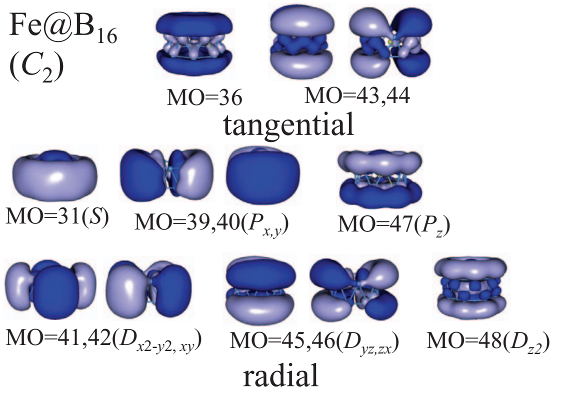

FIG. 3. Canonical molecular orbitals of Fe@B_{16}. The molecular orbital energy level (MO) is marked below each orbital (there is some overlap between the energy levels). B is labeled blue, Fe is labeled yellow.

As shown in Figure 4(b), AdNDP calculation identifies fourteen 3c–2e BBB bonds, three 14c–2e delocalized bonds, and seven 15c–2e delocalized bonds. The three 14c–2e bonds are three tangential delocalized π orbitals in B_{14}. The seven 15c–2e bonds are *spd*-π orbitals formed by *spd* orbitals of Cr and radial delocalized orbitals of B_{14}. Similarly, the seven 15c–2e bonds can be viewed as of super S, $P_{x,y}$, and $D_{xy,yz,xz,x2\text{-}y2}$ orbitals from the orbital symmetry, but the super P_z and D_{z2} orbitals disappear compared with category I. As Cr has got six valence electrons and B_{14} has ten in radial delocalized orbitals, the seven *spd*-π orbitals are occupied with 14 electrons. It does not follow the 18-electrons principle, but why this cluster is stable? The reason may be the flat shape of the compounds, where z direction is much shorter and expanding of orbitals in z direction is difficult. Thus, compared to spherical structures, energy level of super P_z and D_{z2} orbitals will rise up in such a flat structure. To further rise up the energy level of super P_z and D_{z2} orbitals, the thickness of the Cr@B_{14} (1.50 Å) is clearly smaller than that of Ni@B_{14} (1.62 Å), and Cr@B_{14} also has a large HOMO-LUMO gap (2.02 eV) with unoccupied super P_z and D_{z2} orbitals. As a result, although Cr@B_{14} has only seven delocalized *spd*-π orbitals with 14 electrons in radial direction, it also keeps stability due to its special structural shape.

Category III includes Ni@B_{12} and Cr@B_{16}. For Ni@B_{12}, three delocalized π orbitals in the tangential direction and eight delocalized orbitals in the radial direction are obtained in Figure 5(a) by CMO analysis. The tangential π orbitals are also fulfilled with six valence electrons, following the Huckel's rule. And AdNDP results in Figure 5(b) reveal that there are fourteen 3c–2e BBB bonds, three 14c–2e bonds, and eight 15c–2e bonds in this system. The three 14c–2e bonds are tangential delocalized π orbitals. The eight 15c–2e bonds are *spd*-π orbitals (S, $P_{x,y}$, and $D_{xy,yz,xz,x2\text{-}y2,z2}$) formed by *spd* orbitals of Ni and radial delocalized orbitals of B_{12}, occupied with 16 electrons. We identify that there is no super P_z orbital in Ni@B_{12}. As the Cr@B_{14} of category II, delocalized orbitals in z direction should have the relative high energy level in the flat Ni@B_{12} system. So P_z is abandoned to keep the

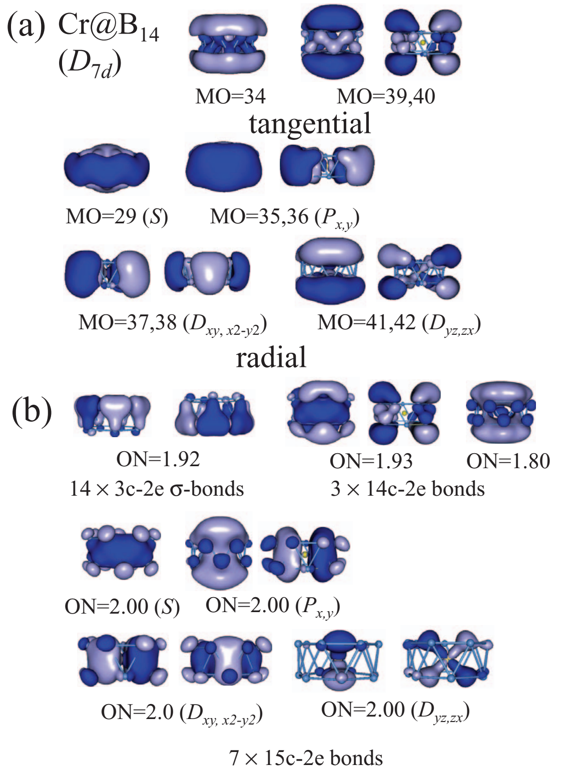

FIG. 4. (a) Canonical molecular orbitals and (b) AdNDP localized bonding patterns of Cr@B_{14}. The molecular orbital energy level (MO) is marked below each orbital (there is some overlap between the energy levels) and occupy number (ON) is marked below each bond. B is labeled blue, Cr is labeled yellow.

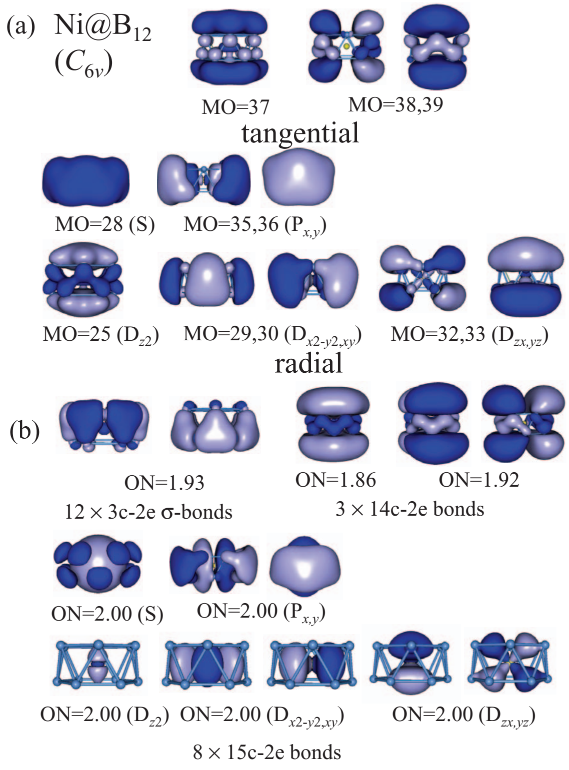

FIG. 5. (a) Canonical molecular orbitals and (b) AdNDP localized bonding patterns of Ni@B_{12}. The molecular orbital energy level (MO) is marked below each orbital (there is some overlap between the energy levels) and occupy number (ON) is marked below each bond. B is labeled blue, Ni is labeled yellow.

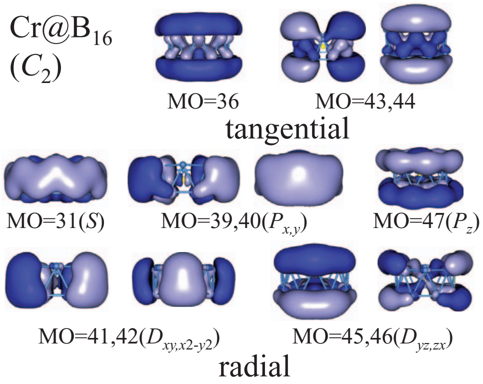

FIG. 6. Canonical molecular orbitals of Cr@B$_{16}$. The molecular orbital energy level (MO) is marked below each orbital (there is some overlap between the energy levels). B is labeled blue, Cr is labeled yellow.

large HOMO-LUMO gap (2.13 eV). But for D_{z2} orbital, it is mainly viewed as d_{z2} lone pairs of Ni, which is hardly influenced by the flat shape of the compound and keeps the low energy level. Consequently, Ni@B$_{12}$ is a stable compound although its radial delocalized *spd*-π orbitals has only 16 electrons which do not follow the 18-electrons principle.

Cr@B$_{16}$ has got the same number of delocalized electrons with Ni@B$_{12}$. Its CMO result plotted in Figure 6 reveals there are three tangential delocalized π orbitals and eight radial delocalized *spd*-π orbitals (S, $P_{x,y,z}$, and $D_{xy,yz,xz,x2\text{-}y2}$) without super D_{z2} orbital. Because the energy level of D_{z2} is relative high as it delocalizes strongly along z direction, it is abandoned to keep the cluster stable. Just as Ni@B$_{12}$ cluster, Cr@B$_{16}$ also has only 16 electrons and does not follow the 18-electrons principle.

For the relative less stable compounds of Fe@B$_{14}$ and Ni@B$_{16}$, the CMO analyses are also used to identify their electronic structures. It is found that Fe@B$_{14}$ has got three delocalized π orbitals in the tangential direction and eight delocalized *spd*-π orbitals in the radial direction (Figure 7(a)). Fe@B$_{14}$ has got the similar electronic structure as Ni@B$_{12}$ with no super P_z orbital, but why it is unstable? The difference is in the super D_{z2} orbital. The super D_{z2} orbital in Ni@B$_{12}$ mainly localizes as the d_{z2} lone pair orbital of Ni, which is influenced little by the molecular shape. However, the super D_{z2} orbital in Fe@B$_{14}$ is a *spd*-π delocalized orbital, which rises up in the flat shape. By analyzing the cation cluster (Fe@B$_{14}$)$^{2+}$, we find that (Fe@B$_{14}$)$^{2+}$ has no D_{z2} orbital compared with Fe@B$_{14}$ and gets a much larger HUMO-LOMO gap (1.81 eV) than the neutral cluster (0.33 eV). Consequently, Fe@B$_{14}$ cluster with occupied D_{z2} orbital loses its stability.

From Figure 7(b), we identify that Ni@B$_{16}$ has four tangential π orbitals and nine radial delocalized *spd*-π orbitals by CMO analysis. Ni@B$_{16}$ has one more occupied tangential π orbital than Ni@B$_{14}$. So it has got eight electrons in tangential orbitals which obeys Huckel's (4n) rule, showing antiaromaticity. As a result, Ni@B$_{16}$ has the small HOMO-LUMO gap (0.84 eV) and its stability is weakened.

From all above, the result of the electronic structure analysis confirms our assumption. The five M@B$_{2n}$ clusters (Ni@B$_{12}$, Cr@B$_{14}$, Ni@B$_{14}$, Cr@B$_{16}$, and Fe@B$_{16}$) have got

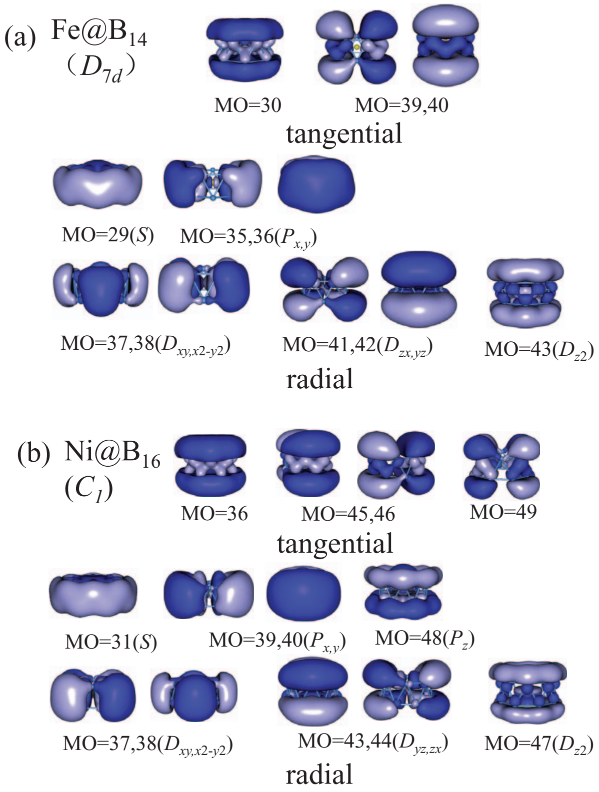

FIG. 7. Canonical molecular orbitals of (a) Fe@B$_{14}$ and (b) Ni@B$_{16}$. The molecular orbital energy level (MO) is marked below each orbital (there is some overlap between the energy levels). B is labeled blue, Fe and Ni are labeled yellow.

delocalized π orbitals in tangential and *spd*-π orbitals in radial directions, showing double aromaticity. They are classified into three categories by different numbers of delocalized orbitals in radial directions and have got different reasons for their stability. This special endohedral bonding pattern is significant in forming the M@B$_{2n}$ clusters.

C. Aromaticity

After analyzing the electronic structure for M@B$_{2n}$, we obtain that each complex get delocalized orbitals in two directions—one perpendicular to the double-ring planar (tangential direction) and one in the double-ring planar (radial direction). Since the delocalization is an important cause of aromaticity, we carry on the study on the aromaticity for these systems. The nucleus independent chemical shift (NICS) has been chosen as the criterion of the aromaticity,[82] in which the negative value means aromaticity and the positive value means antiaromaticity. NICS values at two points of each system (1.5 Å from the central atom upon the ring planar and 1 Å away from the ring side in the radial direction) are calculated and listed in Table II. The negative NICS values at both two points reveal that all compounds in three categories have got double aromaticity. They all have six electrons in three tangential π orbitals which obey the Huckel's ($4n + 2$) rule, showing the planar aromaticity. The number of electrons filling in their radial *spd*-π delocalized orbitals is 18, 14, and 16 for three categories respectively, showing the 3D spherical aromaticity.

TABLE II. The NICS values of Ni@B_{12}, Cr@B_{14}, Ni@B_{14}, Cr@B_{16}, Fe@B_{16}, Ni@B_{16} at two different points (Point 1—1.5 Å from the central atom upon the ring planar and Point 2—1.0 Å away from the ring side in the radial direction).

	$NICS_1$ (ppm)	$NICS_2$ (ppm)
Ni@B_{12}	– 33.1822	– 5.0552
Cr@B_{14}	– 71.4777	– 4.1448
Ni@B_{14}	– 28.3818	– 9.6981
Cr@B_{16}	– 69.0186	– 5.9105
Fe@B_{16}	– 28.3818	– 7.5882
Ni@B_{16}	84.2370	– 18.7541

At last, we study the Ni@B_{16} cluster with small HUMO-LOMO gap (0.84 eV). The NICS values are negative at point 2, but positive at point 1. So Ni@B_{16} shows the antiaromaticity and aromaticity in tangential and radial directions separately, which is different with all the other compounds. So the stability of Ni@B_{16} is weakened, which is in accordance with the result we mentioned in Sec. III B.

IV. CONCLUSION

In this paper, we carry on the theoretical study on the transition metal centered double-ring clusters—M@B_{2n} (M = Ti, Cr, Fe, Ni, Zn, n = 6, 7, 8) using DFT/TPSSh method. The study of structure stability and electronic properties reveals that five of these compounds—Ni@B_{12}, Cr@B_{14}, Ni@B_{14}, Cr@B_{16}, Fe@B_{16} are stable, and they keep their stabilities for three different reasons: (1) Ni@B_{14} and Fe@B_{16} have got three delocalized π orbitals in the tangential direction and nine *spd*-π delocalized orbitals (S, $P_{x,y,z}$, and $D_{xy,yz,xz,x2\text{-}y2,z2}$) in the radial direction, following the Huckel's ($4n + 2$) rule and the 18-electronic principle, respectively. So they have the tangential planar aromaticity and radial spherical aromaticity with the closed-shell structure; (2) Cr@B_{14} have got three delocalized π orbitals in the tangential direction which follows Huckel's ($4n + 2$) rule and seven *spd*-π delocalized orbitals (S, $P_{x,y}$, and $D_{xy,yz,xz,x2\text{-}y2}$) in the radial direction fulfilled with 14 valence electrons. Their P_z and D_{z2} orbitals disappear because of the high energy level of z directional delocalized orbitals in the flat shape. NICS results reveal that they are also the stable structure with double aromaticity. (3) Ni@B_{12} and Cr@B_{16} have got three delocalized π orbitals in the tangential direction and eight *spd*-π delocalized orbitals (S, $P_{x,y}$, and $D_{xy,yz,xz,x2\text{-}y2,z2}$ for Ni@B_{12}, S, $P_{x,y,z}$, and $D_{xy,yz,xz,x2\text{-}y2}$ for Cr@B_{16}) occupied with 16 electrons in the radial direction. Their P_z/D_{z2} orbitals are abandoned because of the high energy level. They are also doubly aromatic and stable.

In the M@B_{2n} clusters, all the *spd*-π delocalized orbitals in radial direction are formed by interaction between the *spd* orbitals in central metal atom and the radial delocalized orbitals in boron ligand. This work reveals the special endohedral bonding model between the metal and boron ligand in the transition metal centered boron double-ring complexes and point out that these clusters are a new class of stable compounds with special double aromaticity. We hope our work will further extend the study on the boron-ligand transition metal systems.

ACKNOWLEDGMENTS

This work is supported by the National Natural Science Foundation of China (Grant No. 21273008), by 211 project of Auhui University. The calculations are carried out on the High-Performance Computing Center of Anhui University. We acknowledge Professor Boldyrev for the AdNDP codes.

[1] T. J. Kealy and P. L. Pauson, Nature (London) **168**, 1039 (1951).
[2] S. A. Miller, J. A. Tebboth, and J. F. Tremaine, J. Chem. Soc. **1952**, 632.
[3] G. Wilkinson, M. Rosenblum, M. C. Whiting, and R. B. Woodward, J. Am. Chem. Soc. **74**, 2125 (1952).
[4] R. B. Woodward, M. Rosenblum, and M. C. Whiting, J. Am. Chem. Soc. **74**, 3458 (1952).
[5] D. Den Boer, P. Den Boer, and H. C. Longuet-Higgins, Mol. Phys. **5**, 387 (1962).
[6] E. M. Shustorovich and M. E. Dyatkina, J. Struct. Chem. **2**, 40 (1961).
[7] A. Haaland, Acta Chem. Scand. **19**, 41 (1965).
[8] R. K. Bohn and A. Haaland, J. Organomet. Chem. **5**, 470 (1966).
[9] A. Haaland and J. Nilsson, Acta Chem. Scand. **22**, 2653 (1968).
[10] J. Brunvoll, S. J. Cyvin, and L. Schäfer, J. Organomet. Chem. **27**, 69 (1971).
[11] K. Warren, Struct. Bond. **27**, 45 (1976).
[12] M. B. Hossain and D. Van der Helm, Inorg. Chem. **17**, 2893 (1978).
[13] J. Weber, M. Geoffroy, A. Goursof, and E. Penigault, J. Am. Chem. Soc. **100**, 3995 (1978).
[14] D. Clack and K. Warren, Struct. Bond. **39**, 1 (1980).
[15] A. Chistyakov, J. Struct. Chem. **26**, 833 (1985).
[16] V. A. Piven and Y. S. Nekrasov, Russ. Chem. Bull. **36**, 1526 (1987).
[17] C. Elschenbroich, J. Hurley, B. Metz, W. Massa, and G. Baum, Organomet. **9**, 889 (1990).
[18] L. Phillips and G. R. Dennis, J. Chem. Soc. Dalton Trans. **1995**, 1469.
[19] C. Elschenbroich, E. Schmidt, R. Gondrum, B. Metz, O. Burghaus, W. Massa, and S. Wocadlo, Organomet. **16**, 4589 (1997).
[20] J. Ruiz, F. Ogliaro, J. Y. Saillard, J. F. Halet, F. Varret, and D. Astruc, J. Am. Chem. Soc. **120**, 11693 (1998).
[21] G. Y. Hong, M. Dolg, and L. Li, Int. J. Quantum Chem. **80**, 201 (2000).
[22] J. Aihara, J. Phys. Chem. A **105**, 5486 (2001).
[23] Q. S. Li and H. W. Jin, J. Phys. Chem. A. **106**, 7042 (2002).
[24] C. L. Yang, Z. H. Zhang, T. Q. Ren, R. Wang, and Z. H. Zhu, J. Mol. Struct. (THEOCHEM) **583**, 63 (2002).
[25] Z. F. Xu, Y. Xie, W. L. Feng, and H. F. Schaefer, J. Phys. Chem. A **107**, 2716 (2003).
[26] S. Chacko, D. Kanhere, and I. Boustani, Phys. Rev. B **68**, 035414 (2003).
[27] H. W. Jin and Q. S. Li, Phys. Chem. Chem. Phys. **5**, 1110 (2003).
[28] Q. S. Li and Q. Jin, J. Phys. Chem. A **107**, 7869 (2003).
[29] Q. S. Li, Q. Jin, Q. Luo, A. C. Tang, J. K. Yu, and H. X. Zhang, Int. J. Quantum Chem. **94**, 269 (2003).
[30] J. Ma, Z. H. Li, K. N. Fan, and M. F. Zhou, Chem. Phys. Lett. **372**, 708 (2003).
[31] V. M. Rayon and G. Frenking, Organomet. **22**, 3304 (2003).
[32] S. J. Xu, J. Nilles, D. Radisic, W. J. Zheng, S. Stokes, K. H. Bowen, R. C. Becker, and I. Boustani, Chem. Phys. Lett. **379**, 282 (2003).
[33] Q. S. Li and L. F. Gong, J. Phys. Chem. A **108**, 4322 (2004).
[34] S. D. Li, J. C. Guo, C. Q. Miao, and G. M. Ren, Angew. Chem. Int. Ed. **44**, 2158 (2005).
[35] L. L. Pan, J. Li, and L. S. Wang, J. Chem. Phys. **129**, 024302 (2008).
[36] T. N. Gribanova, A. G. Starikov, R. M. Minyaev, V. I. Minkin, M. R. Siebert, and D. J. Tantillo, Chem. Eur. J. **16**, 2272 (2010).
[37] J. J. Zhao, L. Wang, F. Y. Li, and Z. F. Cheng, J. Phys. Chem. A **114**, 9969 (2010).
[38] L. M. Wang, B. B. Averkiev, J. A. Ramilowski, W. Huang, L. S. Wang, and A. I. Boldyrev, J. Am. Chem. Soc. **132**, 14104 (2010).
[39] E. Maslowsky, Coord. Chem. Rev. **255**, 2746 (2011).
[40] C. H. Wang, L. F. Xu, X. L. Fan, and J. T. Wang, Phys. Lett. A **375**, 562 (2011).
[41] Z. A. Piazza, W. L. Li, C. Romanescu, A. P. Sergeeva, L. S. Wang, and A. I. Boldyrev, J. Chem. Phys. **136**, 104310 (2012).
[42] E. Urneúzÿius, W. W. Brennessel, C. J. Cramer, J. E. Ellis, and P. R. Schleyer, Science **295**, 832 (2002).

[43] H. J. Zhai, L. S. Wang, A. N. Alexandrova, and A. I. Boldyrev, J. Chem. Phys. **117**, 7917 (2002).

[44] H. J. Zhai, B. Kiran, J. Li, and L. S. Wang, Nat. Mater. **2**, 827 (2003).

[45] A. N. Alexandrova, A. I. Boldyrev, H. J. Zhai, L. S. Wang, E. Steiner, and P. W. Fowler, J. Phys. Chem. A **107**, 1359 (2003).

[46] H. J. Zhai, A. N. Alexandrova, K. A. Birch, A. I. Boldyrev, and L. S. Wang, Angew. Chem. Int. Ed. **42**, 6004 (2003).

[47] H. J. Zhai, L. S. Wang, A. N. Alexandrova, A. I. Boldyrev, and V. G. Zakrzewski, J. Phys. Chem. A **107**, 9319 (2003).

[48] A. C. Tsipis and A. T. Chaviara, Inorg. Chem. **43**, 1273 (2004).

[49] A. N. Alexandrova, H. J. Zhai, L. S. Wang, and A. I. Boldyrev, Inorg. Chem. **43**, 3552 (2004).

[50] A. N. Alexandrova, A. I. Boldyrev, H. J. Zhai, and L. S. Wang, J. Phys. Chem. A **108**, 3509 (2004).

[51] A. N. Alexandrova, A. I. Boldyrev, H. J. Zhai, and L. S. Wang, Coord. Chem. Rev. **250**, 2811 (2006).

[52] H. J. Zhai, L. S. Wang, D. Y. Zubarev, and A. I. Boldyrev, J. Phys. Chem. A **110**, 1689 (2006).

[53] H. J. Zhai, C. Q. Miao, S. D. Li, and L. S. Wang, J. Phys. Chem. A **114**, 12155 (2010).

[54] W. Huang, A. P. Sergeeva, H. J. Zhai, B. B. Averkiev, L. S. Wang, and A. I. Boldyrev, Nat. Chem. **2**, 202 (2010).

[55] B. Kiran, S. Bulusu, H. J. Zhai, S. Yoo, X. C. Zeng, and L. S. Wang, Proc. Natl. Acad. Sci. U.S.A. **102**, 961 (2005).

[56] A. P. Sergeeva, I. A. Popov, Z. A. Piazza, W. L. Li, C. Romanescu, L. S. Wang, and A. I. Boldyrev, Acc. Chem. Res. **47**, 1349 (2014).

[57] H. T. Pham, L. V. Duong, B. Q. Pham, and M. T. Nguyen, Chem. Phys. Lett. **577**, 32 (2013).

[58] I. A. Popov, Z. A. Piazza, W. L. Li, L. S. Wang, and A. I. Boldyrev, J. Chem. Phys. **139**, 144307 (2013).

[59] L. Cheng, J. Chem. Phys. **136**, 104301 (2012).

[60] T. B. Tai, L. V. Duong, H. T. Pham, D. T. T. Maia, and M. T. Nguyen, Chem. Commun. **50**, 1558 (2014).

[61] C. Romanescu, T. R. Galeev, W. L. Li, A. I. Boldyrev, and L. S. Wang, Angew. Chem. Int. Ed. **50**, 9334 (2011).

[62] C. Romanescu, A. P. Sergeeva, W. L. Li, A. I. Boldyrev, and L. S. Wang, J. Am. Chem. Soc. **133**, 8646 (2011).

[63] W. L. Li, C. Romanescu, T. R. Galeev, Z. A. Piazza, A. I. Boldyrev, and L. S. Wang, J. Am. Chem. Soc. **134**, 165 (2012).

[64] C. Romanescu, T. R. Galeev, A. P. Sergeeva, W. L. Li, L. S. Wang, and A. I. Boldyrev, J. Organomet. Chem. **721**, 148 (2012).

[65] T. R. Galeev, C. Romanescu, W. L. Li, L. S. Wang, and A. I. Boldyrev, Angew. Chem. Int. Ed. **51**, 2101 (2012).

[66] S. D. Li, C. Q. Miao, J. C. Guo, and G. M. Ren, J. Comput. Chem. **27**, 1858 (2006).

[67] Q. Chen and S. D. Li, J. Cluster Sci. **22**, 513 (2011).

[68] Y. Yuan and L. Cheng, J. Chem. Phys. **138**, 024301 (2013).

[69] I. A. Popov, W. L. Li, Z. A. Piazza, A. I. Boldyrev, and L. S. Wang, J. Phys. Chem. A **118**(37), 8098 (2014).

[70] Y. Yuan and L. Cheng, J. Chem. Phys. **137**, 044308 (2012).

[71] W. An, S. Bulusu, Y. Gao, and X. C. Zeng, J. Chem. Phys. **124**, 154310 (2006).

[72] M. P. Johansson, J. Phys. Chem. C **113**, 524 (2009).

[73] B. Kiran, G. G. Kumar, M. T. Nguyen, A. K. Kandalam, and P. Jena, Inorg. Chem. **48**, 9965 (2009).

[74] J. Tao, J. P. Perdew, V. N. Staroverov, and G. E. Scuseria, Phys. Rev. Lett. **91**, 146401 (2003).

[75] L. Li, C. Xu, and L. Cheng, Comput. Theor. Chem. **1021**, 144 (2013).

[76] L. F. Li and L. J. Cheng, J. Chem. Phys. **138**, 094312 (2013).

[77] M. J. Frisch, G. W. Trucks, H. B. Schlegel *et al.*, Gaussian 09, Revision B.01, Gaussian, Inc., Wallingford, CT, 2009.

[78] U. Varetto, Molekel 5.4.0.8, Swiss National Supercomputing Centre, Manno, Switzerland.

[79] D. E. Bean and P. W. Fowler, J. Phys. Chem. C **113**, 15569 (2009).

[80] D. Y. Zubarev and A. I. Boldyrev, Phys. Chem. Chem. Phys. **10**, 5207 (2008).

[81] T. R. Galeev, B. D. Dunnington, J. R. Schmidt, and A. I. Boldyrev, Phys. Chem. Chem. Phys. **15**, 5022 (2013).

[82] P. R. Schleyer, C. Maerker, A. Dransfeld, H. J. Jiao, and N. J. R. E. Hommes, J. Am. Chem. Soc. **118**, 6317 (1996).